

**RELATÓRIO DE ATIVIDADES DESENVOLVIDAS
SEMESTRE 2020.1**

CAMPUS: PESQUEIRA	COORDENAÇÃO Edificações	
PROFESSOR: Ruan Landolfo da Silva Ferreira	GRUPO I	REGIME DE TRABALHO: () 20h () 40h (X) DE

TODAS AS ATIVIDADES DESENVOLVIDAS DEVERÃO SER COMPROVADOS (ART. 21)

ATIVIDADES DE ENSINO				
COMPONENTES CURRICULARES	CURSO	C.H. TOTAL DO COMPONENTE	C.H. SEMANAL	C.H. de PREPARAÇÃO DE AULAS
A12-PS.081 - MATERIAIS DE CONSTRUÇÃO I	Edificações Médio Integrado	40,5	2,25	2,25
A12-PS.085 - TECNOLOGIA DA CONSTRUÇÃO I	Edificações Médio Integrado	40,5	2,25	2,25
A12-PS.092 - TECNOLOGIA DA CONSTRUÇÃO III	Edificações Médio Integrado	54	3,0	3,0
A12-PS.097 - MÁQUINAS E EQUIPAMENTOS	Edificações Médio Integrado	27	1,5	1,5
A12-PS.104 - MANUTENÇÃO PREDIAL	Edificações Médio Integrado	27	1,5	1,5
SUBTOTAL		189	10,5	10,5
ATIVIDADE				C.H. Semanal
PARTICIPAÇÃO EM REUNIÕES SEMANAIS DE PLANEJAMENTO PEDAGÓGICO				2,0
GRAVAÇÃO DE VIDEOAULAS PARA O ATENDIMENTO AOS DISCENTES EM PLATAFORMA PROPÍCIA PARA O ENSINO REMOTO				2,0
ORGANIZAÇÃO DE EVENTOS, EM CONJUNTO COM ESTUDANTES DO IFPE, TAIS COMO CONGRESSOS, SEMINÁRIOS, COLÓQUIOS E AFINS, DIRECIONADOS AO CORPO DISCENTE DA INSTITUIÇÃO (EDIFLIVE)				2,0
ORIENTAÇÃO DE ESTÁGIO – ALUNO(A)S: ANA BEATRIZ NUNES LEAL E MARCO ANTÔNIO BARBOSA DA SILVA				4,0

ATIVIDADES DE PESQUISA	
ATIVIDADE	C.H. Semanal
PUBLICAÇÃO DE ARTIGOS CIENTÍFICOS EM REVISTAS INDEXADAS - Fernandes, C. N., Ferreira, R. L., Bernardo, R. D., Avelino, F., & Bertini, A. A. (2020). Using TiO ₂ nanoparticles as a SO ₂ catalyst in cement mortars. <i>Construction and Building Materials</i> , 257, 119542.	4,0



ATIVIDADES DE EXTENSÃO
PARTICIPAÇÃO COMO COLABORADOR EM PROJETO DE EXTENSÃO INTITULADO POR “DESENVOLVIMENTO SUSTENTÁVEL NAS CONSTRUÇÕES DO POVO INDÍGENA XUKURU DO ORORUBÁ: ENSINO E APRENDIZAGEM POR MEIO DE REGISTROS E INFORMAÇÕES DO POVO XUKURU” – C.H. SEMANAL: 2,0

ATIVIDADES ADMINISTRATIVO-PEDAGÓGICAS
--

ATIVIDADE	C.H. Semanal
COMISSÃO DE REESTRUTURAÇÃO PPC EDFICIAÇÕES MÉDIO INTEGRADO E SUBSEQUENTE. DECLARAÇÃO CACC/DENS/IFPE – PESQUEIRA. PORTARIA Nº 057/2014 - DGCP05/2020	3,0

COMPLEMENTO / OBSERVAÇÕES

DISTRIBUIÇÃO DA CARGA HORÁRIA						
AULAS	PREPARAÇÃO DE AULAS	APOIO AO ENSINO	PESQUISA	EXTENSÃO	ADMINISTRATIVO PEDAGÓGICO	TOTAL/SOMA
10,5	10,5	11,0	4,0	2,0	3,0	40

<p>Documento assinado digitalmente</p> <p> Ruan Landolfo da Silva Ferreira Data: 14/11/2020 13:40:28-0300 CPF: 076.888.504-36</p>	<p>Documento assinado digitalmente</p> <p> Jose Denis Gomes Lima da Silva Data: 15/11/2020 06:28:12-0300 CPF: 048.249.324-08</p>	
_____	_____	_____
DOCENTE	COORDENAÇÃO	DEPARTAMENTO

_____	_____	_____
DIREÇÃO DE PESQUISA	DIREÇÃO DE EXTENSÃO	DIREÇÃO DE ENSINO



SERVIÇO PÚBLICO FEDERAL
MINISTÉRIO DA EDUCAÇÃO
SECRETARIA DE EDUCAÇÃO PROFISSIONAL E TECNOLÓGICA
INSTITUTO FEDERAL DE EDUCAÇÃO, CIÊNCIA E TECNOLOGIA DE PERNAMBUCO
CAMPUS PESQUEIRA

COORDENAÇÃO DA ÁREA DE CONSTRUÇÃO CIVIL - CACC

DECLARAÇÃO

Declaro para comprovação junto ao IFPE que os professores citados na tabela abaixo, participaram de 20 reuniões regulares para o planejamento pedagógico da Coordenação da Área de Construção Civil, no período 22/02/2020 à 24/11/2020.

Docentes	Siape
ELÂNIA DE SOUZA MELO	1650623
ISNARD FERREIRA DA SILVA	1204757
JAQUELINE MATIAS DA SILVA	1397823
JOSE DENIS GOMES LIMA DA SILVA	1971579
JOSE MARIA DE ARAUJO	1229245
MANUELA QUEIROZ OLIVEIRA	2891298
MARCOS ANTONIO ARRUDA G. DE HOLANDA	1217759
MARIO JOSE RIBEIRO DA SILVA	1216014
RAFAEL RONEY CAMARA DE MELO	1959798
RICARDO GOMES FREIRE DUARTE	3131891
RONALDO ALVES DE OLIVEIRA FILHO	2961669
RUAN LANDOLFO FERREIRA DA SILVA	3087909

Pesqueira, 13 de novembro de 2020.



Documento assinado digitalmente

Jose Denis Gomes Lima da Silva

Data: 13/11/2020 11:08:55-0300

CPF: 048.249.324-08

José Denis Gomes Lima da Silva / Siape 1971579
Coordenador da Área de Construção Civil
IFPE Campus Pesqueira



SERVIÇO PÚBLICO FEDERAL
MINISTÉRIO DA EDUCAÇÃO
SECRETARIA DE EDUCAÇÃO PROFISSIONAL E TECNOLÓGICA
INSTITUTO FEDERAL DE EDUCAÇÃO, CIÊNCIA E TECNOLOGIA DE PERNAMBUCO
CAMPUS PESQUEIRA

COORDENACÃO DA ÁREA DE CONSTRUÇÃO CIVIL - CACC

DECLARAÇÃO

Declaro para comprovação junto ao IFPE que os professores citados na tabela abaixo, organizaram a o evento EDIFLIVE, no período 20/05/2020 à 01/07/2020 de forma remota e com participação do público discente e externo ao IFPE.

Docentes	Siape
ELÂNIA DE SOUZA MELO	1650623
ISNARD FERREIRA DA SILVA	1204757
JAQUELINE MATIAS DA SILVA	1397823
JOSE DENIS GOMES LIMA DA SILVA	1971579
JOSE MARIA DE ARAUJO	1229245
MANUELA QUEIROZ OLIVEIRA	2891298
MARCOS ANTONIO ARRUDA G. DE HOLANDA	1217759
MARIO JOSE RIBEIRO DA SILVA	1216014
RAFAEL RONEY CAMARA DE MELO	1959798
RICARDO GOMES FREIRE DUARTE	3131891
RONALDO ALVES DE OLIVEIRA FILHO	2961669
RUAN LANDOLFO FERREIRA DA SILVA	3087909

Pesqueira, 13 de novembro de 2020.



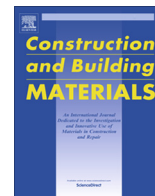
Documento assinado digitalmente

Jose Denis Gomes Lima da Silva

Data: 13/11/2020 11:07:43-0300

CPF: 048.249.324-08

José Denis Gomes Lima da Silva / Siape 1971579
Coordenador da Área de Construção Civil
IFPE Campus Pesqueira



Using TiO₂ nanoparticles as a SO₂ catalyst in cement mortars

Cristiane N. Fernandes^{a,*}, Ruan L.S. Ferreira^{b,*}, Ricardo D.S. Bernardo^c, Francisco Avelino^d, Alexandre A. Bertini^a

^a Federal University of Ceará, Technology Center, Structural Engineering and Building Construction Department, PICI Campus, 60455900 Fortaleza, Brazil

^b Federal Institute of Education, Science and Technology of Pernambuco, Civil Construction Department, 55200-000 Pesqueira, Brazil

^c Ceará State University, Crateús School of Education, 63700000 Crateús, Brazil

^d Federal Institute of Education, Science and Technology of Ceará, Biopolymers and Advanced Materials Group, 63503790 Iguatu, Brazil

HIGHLIGHTS

- Mortars with TiO₂ incorporation (2.5–10%) were produced.
- The effect of adding TiO₂ on the mortars physical–mechanical properties was evaluated.
- The incorporation of TiO₂ in mortars in the degradation process of SO₂ was investigated.
- The nano-TiO₂ decontaminated the samples previously contaminated by the pollutant SO₂.

ARTICLE INFO

Article history:

Received 11 December 2019

Received in revised form 6 May 2020

Accepted 11 May 2020

Keywords:

Nanomaterials
Titanium dioxide
Buildings
Atmospheric pollution
Photocatalysis
Cementitious materials

ABSTRACT

Titanium dioxide (TiO₂) has been used in building materials to produce products that do not require major maintenance and also contribute to improve air quality and extend the life of buildings. Thus, this research evaluated the effects of incorporation of this substance into cement mortars in the process of degradation of sulfur dioxide (SO₂), one of the largest atmospheric pollutants. Mortars were developed at a weight ratio of 1:3 (cement: sand), incorporating 2.5%, 5%, 7.5% and 10% of TiO₂ relative to the cement weight. Mortars were evaluated in their fresh state (consistency and bulk density) and hardened (dry bulk density, water absorption by capillarity, open porosity and flexural and compressive strength). The samples were exposed to an accelerated aging SO₂ (pollutant) chamber, then moistened and exposed to ultraviolet radiation. For this exposure of the samples, two Light Emitter Diodes (LEDs) with wavelengths covering the UV-A range were used: UV (380–420 nm) and blue (420–493 nm). Fourier Transform Infrared measurements were also performed in three stages, which were: (1) before contamination, (2) after SO₂ contamination and (3) after radiation exposure. The nano TiO₂ incorporation in the mortars contributed to the increase in open porosity and favored the increase in dry bulk density of mortars this was due to the filler effect. In addition, there was an increase in both the compressive strength and the flexural strength for mortars with addition, compared with the reference mortar. It can be concluded that the incorporation of TiO₂ improved the physical, mechanical and photocatalytic properties, and enabled the decontamination of mortars due to the action of the SO₂ pollutant.

© 2020 Elsevier Ltd. All rights reserved.

1. Introduction

Air pollution is due to the discharge of harmful substances into the atmosphere [1], which cause adverse effects especially in large cities. The problems related to this type of pollution in urban areas have been known for a long time [2]. About 3000 distinct compounds have been identified, most of them organic [3].

Among the main air pollutants are carbon monoxide (CO), nitrogen oxides (NO_x), sulfur dioxide (SO₂), ozone (O₃), soot and particulate matter, represented by inhalable particles and in suspension [4]. The main degrading agents of constructions are the SO_x and NO_x [5]. In addition to affecting human health [6] and contributing to increased air pollution, these pollutants contribute to the emergence of pathological manifestations due to the incorporation of pollutants into building facades.

In 116 cities in China (the most populous city in the world), increased industrial SO₂ emissions were found to account for a 3.5% increase in the number of lung cancer patients, as well as

* Corresponding authors.

E-mail addresses: cristiane_nascimento_fernandes@outlook.com (C.N. Fernandes), ruan_landolfo@hotmail.com (R.L.S. Ferreira).

an increase of 3% in mortality from respiratory diseases, causing the death of about one hundred thousand people a year [7]. These statistical data demonstrate the need to study ways to mitigate the effects caused by SO₂ pollutant. Some substances have been discovered and used to enable the reduction in negative impacts caused to the environment by polluting agents, and one of these is the titanium dioxide (TiO₂).

This nanomaterial is considered by many researchers to be an excellent agent in the degradation of pollutants found in atmospheric [8–10] and wastewater [11] due to its high oxidizing and reducing abilities [12]. When a TiO₂ material is irradiated by sunlight, its surface creates a barrier capable of retarding the rate of contamination of the underlying surfaces [10] due to the mineralization of polluting agents (organic and inorganic) through oxidation–reduction reaction [13], which may in particular be described as a photocatalytic process [14]. Harmful pollutants (such as NO_x and SO_x) are converted into less toxic forms and subsequently leached by rain [14,15]. As a result, the service life of buildings is extended and consequently the costs related to maintenance operations are reduced.

The TiO₂ is a photocatalyst that has more than one crystalline phase, and the main ones are: rutile, anatase and brookite [16]. Anatase and rutile have tetragonal structures. The brookite phase is orthorhombic in nature [17]. Brookite is a phase of TiO₂ that is not given much attention in terms of its properties and applications. This is due to the difficulty of producing pure particles from this phase. [18]. The most well-known phases used in building materials are rutile and anatase [19]. As anatase has the greatest photocatalytic effect [20], it is the most used phase in studies incorporating TiO₂ into building materials, whose main objective is to increase the useful life of buildings.

Thus, the worldwide scientific and industrial interest in this substance for the most diverse civil engineering applications has become clear [8]. Studies on the use of nano-TiO₂ have been developed for: air purification [21], asphalt pavement protection with NO₂ degradation [22], photocatalytic degradation of tetracycline-containing wastewater [23], degradation of wood pollutants [24], asphalt shingle [25], cementitious materials [13,26–33] (which is the focus of this study, in mortars) and others.

Incorporating TiO₂ nanoparticles in mortars can improve their mechanical properties due to the modification of their microstructure [31] and, consequently, help to increase their durability [34]. Studies on the use of TiO₂ nanoparticles in cement composites also show that these nanoparticles have a nucleation effect on the cement paste [34], which contributes to a better distribution of hydration products and to the formation of stronger clusters of C-S-H [35] in the microstructure of cementitious materials.

In recent years, there has been an increasing number of studies related to the use of TiO₂ in cementitious materials. However, some factors contribute to the effects of adding TiO₂ in mortars, which are not fully clarified. Firstly, studies concerning the synergistic effects of adding TiO₂ to the physical–mechanical and photocatalytic properties of mortars are scarce, which limits the obtaining of information that contributes to fill the existing gaps on the subject. Second, because the number of studies investigating the effects of SO₂ is also limited, despite the importance of minimizing environmental impacts. Finally, although there are studies [19,36–45] with optical or morphological analyses of TiO₂, there is also a very limited number of studies applied to construction materials, as there is little association between these evaluations and a physical investigation of the material. These aspects mentioned above need to be evaluated so that the existing gaps on the topic can be filled. Therefore, this study assesses the effects of TiO₂ incorporation on the physical, mechanical and photocatalytic properties of Portland cement-based mortars contaminated with SO₂.

2. Materials and methods

2.1. Materials

In this research, Brazilian Pozzolan Portland cement (PC) (similar to ASTM C 595 Portland Pozzolan) was used, with a density of 2.96 g/cm³, a bulk density of 1.14 kg/dm³, a specific surface of 0.44 m²/g, and compressive strength of 32 MPa at 28 days. Silica sand obtained from the riverbed was used as an aggregate. This sand had a specific density of 2.61 g/cm³, a unit mass of 1.4 kg/dm³, a maximum diameter of 2.36 mm and a fineness modulus of 2.4.

The titanium dioxide (TiO₂) powder was commercially obtained from COREMAL S/A, with 99.5% purity and a specific mass of 3800 kg/m³. The characterization for X-Ray Diffraction (XRD) was performed in the range of 20° to 90°, in 2θ, with a step size of 0.05° and time per step of 1 s, with the samples in powder form. (Fig. 1). For refinement, the Rietveld method was used. The readings were taken with radiation K-α of cobalt in the range 2θ/second of 20° to 90°. The diameter equivalent of the TiO₂ particles is 60.64 ± 3.71 nm. This result is consistent with previous studies whose average TiO₂ particle diameter ranged from 532 to 40 nm [27,46–48].

2.2. Composition and manufacturing

The following criteria were established for the production of mortars:

- Produce mortars with a 1:3 (cement:dry sand) in weight.
- Replace PC by weight with TiO₂ percentages of 2.5%, 5%, 7.5% and 10%. The high levels of TiO₂ used in this work are due to the greater effect on the degradation of SO₂ gas. In addition, these dosage levels are compatible with previous studies [30].
- Produce mortars with flow within the range of 260 ± 5 mm, based on the consistency table test and the criteria established by the Brazilian standard NBR 13276: 2016 (similar to ASTM C1329/C1329M: 2016). The ideal amount of water for mixing the mortars was experimentally adjusted to strictly guarantee the specified workability.
- The mortars were mixed in a standard mechanical mixer according to the procedure described by Brazilian Standard NBR 16541:2016.

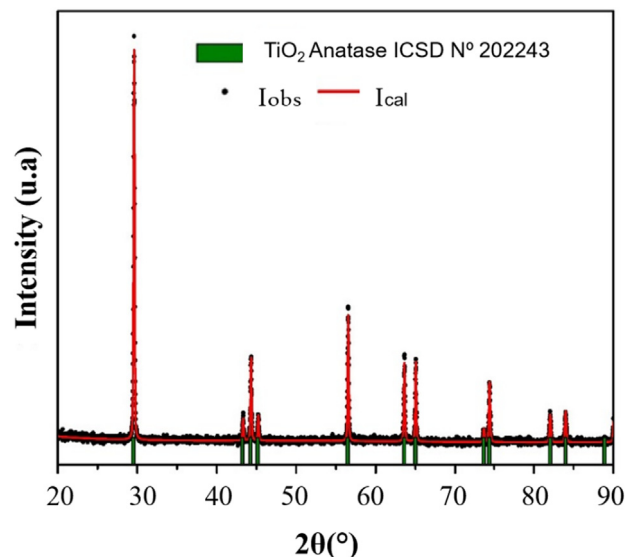


Fig. 1. XRD of TiO₂ (anatase).

Table 1
Composition of the mortar mixes (kg/m³).

Mortar	%TiO ₂	Cement	Sand	TiO ₂	Water
M0 (Control)	0	750	2250	0	485
M1	2.5	750	2250	18.75	500
M2	5.0	750	2250	37.5	500
M3	7.5	750	2250	56.25	500
M4	10	750	2250	75.00	515

The percentage of PC substitution by TiO₂ was suffixed, where each series is presented by the substituted percentage. For example, a mixing ratio with 2.5% TiO₂ is a series, namely M1. Thus, five series were established and the compositions of the materials used to produce 1 m³ of mortar are shown in Table 1.

2.3. Tests on mortar mixes

The methods used in the tests to evaluate the physical, mechanical and photocatalytic properties of mortars are shown below in Table 2. The samples were submitted to the following curing conditions: dry curing and in laboratory with relative humidity of 95 ± 5% and a temperature of 20 ± 2 °C for 2 days within the molds. After demoulding, the samples were kept in the same conditions mentioned above until the age of the physical and mechanical tests shown in Table 2.

Table 2
Tests performed on mortars and their respective methods and standards.

Properties	Standard	Specimens and size	Curing time (days)
Properties of fresh mortar			
Consistence by flow table	NBR 13276:2016 ¹	3	–
Bulk density	NBR 13278:2005 ²	3	–
Properties of hardened mortar			
Dry bulk density	NBR 13280:2005 ³	3 Prismatic (40x40x160 mm)	28
Water absorption by capillarity	NBR 15259:2005 ⁴	3 Prismatic (40x40x160 mm)	28
Open porosity	NBR 9778:2009 ⁵	3 Prismatic (40x40x160 mm)	28
Compressive strength	NBR 13279:2005 ⁶	6 Prismatic (40 × 40 × 80 mm)	7 and 28
Flexural strength	NBR 13279:2005 ⁷	3 Prismatic (40x40x160 mm)	7 and 28

Equivalent to: ¹EN 1015–3 (1999); ²EN 1015–6:1998; ³EN 1015–10:1999; ⁴EN 1015–18: 2002; ⁵NP EN 1936:2007; ^{6,7}EN 1015–11:1999.

2.4. Photocatalytic properties

The prepared samples were exposed to the pollutant SO₂ in a chamber for accelerated industrial corrosion testing model UK-01 for a 24-hour machine cycle. The mortar compositions were exposed for 8 h to SO₂ inside the closed chamber, at a relative humidity of 20 ± 5. Then, they remained 16 h inside the open chamber. The degradation of organic compounds or pollutants occurs under the effect of humidity and UV radiation [10], where the pollution control mechanism is activated within a UV-A range [28], which comprises a wavelength (λ) of 320–400 nm [49].

Thus, the mortars were moistened and then KBr (potassium bromide) pellets were generated. A 2 mg sample was generated for each mortar composition and all samples were subjected to UV radiation. The pellets were placed in a centralized support inside the experimental box. The light wattage of the LEDs has of 65 W. To expose the pieces, two Light-Emitting Diodes (LEDs) (Fig. 2) with wavelengths that cover the UV-A range were used: UV (380–420 nm) and blue (420–493 nm). The LEDs were selected to ensure that the UV-A range was reached (Table 3). Two LEDs were used as a safety margin for this.

Infrared spectra were generated in a Shimadzu IRTracer-100 spectrophotometer in the range of 400 to 4000 cm⁻¹ for each mortar type in three stages. The stages considered were: (1) before contamination, (2) after SO₂ contamination and (3) after radiation exposure. For this, one sample was used for each stage of each mortar produced, totaling 3 samples per type of mortar. This whole procedure was performed to prove the contamination of the sample through the behavior of the main bands of the elements present in the composition.

Then the spectra were generated in a FTLA 2000–102, ABB-MAN spectrophotometer, also in the region of 400 to 4000 cm⁻¹, but with an enlargement of the graph in the region of vibration related to SO₂. This localization was observed by the behavior of the previously obtained bands. This was done to verify for possible reductions in the amount of sulfur in the material. Verifying the reduction aims to show the decontamination of the parts with the addition of TiO₂ due to exposure to radiation for 100 min.

Table 3
Wavelength ranges of LEDs [50].

LED	Wavelength (nm)
UV	380 – 420
Blue	420 – 493
Green	484 – 581
Yellow	563 – 616
Red	594 – 659

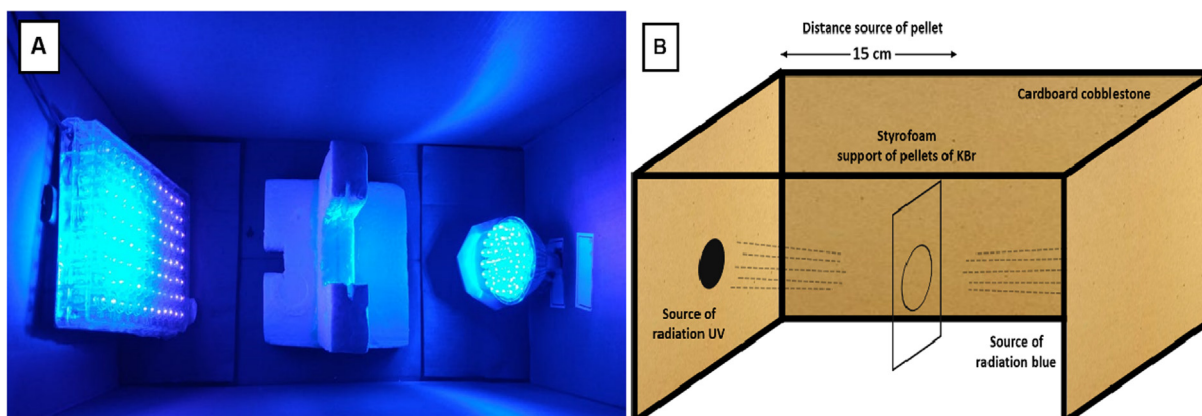


Fig. 2. Experimental apparatus for exposure to UV radiation (a) LEDs in operation (b) layout with material specifications.

3. Results and discussion

3.1. Properties of fresh mortar

3.1.1. Consistency

The consistency test (Table 4) was performed to quantify the water content to be added to the mortar, based on the consistency values set in the dispersion range of 260 ± 5 mm. In addition, it was important to set this parameter to ensure proper workability and to improve the mortar comparability.

The incorporation of TiO_2 resulted in a reduction in the water content/fines to maintain the same workability. The reason for this is due to the filling effect. The TiO_2 nanoparticles filled the voids between the sand particles and, as a result, the amount of water required for mixing was also reduced. On the other hand, increasing the content of nano- TiO_2 resulted in the reduction of workability, therefore water content had to be increased to maintain the same workability. This is due to the high surface area of the nano- TiO_2 that absorbs more water and also the non-dissolution in water of the nano- TiO_2 particles [31]. These results are consistent with those obtained by Noorvand et al. [51] and show that using higher TiO_2 contents contributes to the refinement of the porous structure of mortars and the amount of water in the mixture is substantially reduced. However, this phenomenon was different from the study by Hüsken et al. [28]. This is believed to be due to the fact that the authors added TiO_2 dissolved in water, while in our study we used TiO_2 mixed with cement for incorporation.

3.1.2. Bulk density

Although TiO_2 nanoparticles have a lower bulk density compared to cement and sand, the bulk density of mortars increased

Table 4
Consistency of the mortars.

Mortar	Consistency (mm)	water/cement	water/fines ^a
M0	262	0.65	0.65
M1	265	0.67	0.65
M2	263	0.67	0.63
M3	260	0.67	0.62
M4	260	0.69	0.62

^a water/(cement + TiO_2) ratio

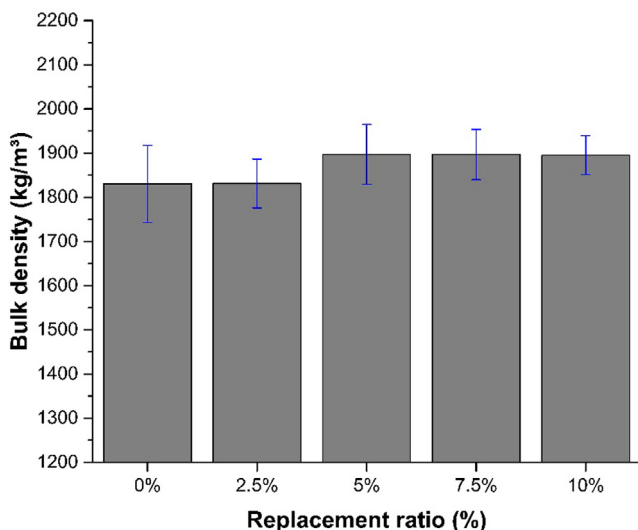


Fig. 3. Bulk density of fresh mortar.

slightly to levels of TiO_2 incorporation above 2.5% (Fig. 3). However, the largest amount of fine particles fills the voids between the larger particles and those that would be occupied by water. The filling effect provided by the TiO_2 particles results in greater compaction of the mixture and, therefore, increases the bulk density.

The values found show that all mortars can be used for decorative monolayer coating, as they have a fresh bulk density between 1800 and 2200 kg/m^3 , established by the NBR 13281:2005 Brazilian standard.

3.2. Properties of hardened mortar

3.2.1. Dry bulk density

Overall, dry bulk density results (Fig. 4) did not follow the same trend as in the fresh state. However, the incorporation of TiO_2 favored the increase of dry bulk density of mortars, except when the content was 7.5% (M3). This was due to the filler effect. For mortar M3, the mixing was probably performed inefficiently resulting in agglomeration of TiO_2 particles and, consequently, increased internal voids when the mortar became hardened.

3.2.2. Water absorption by capillarity

To analyze the results of the tests for water absorption by capillary at 28 days (Fig. 5) was used as parameter the capillary coefficient. The capillary coefficient was calculated using the mass of water absorbed between 10 and 90 min, per area unit and square root of time. Thus, the parameter indicates the rate of water absorbed due to capillary rise in the first minutes of testing.

The capillary coefficient of mortars produced with TiO_2 decreases when compared to the reference mortar (M0). Certainly, the volume of capillary pores was reduced by incorporating a larger volume of very fine particles, which resulted in improved water absorption behavior of mortars. Another reason why the capillary water absorption of mortars was reduced using nano TiO_2 is due to the fact that the TiO_2 nanoparticles increase the content of the chemically combined water due to the higher hydration rate. As a result of this process, unbound water and, consequently, capillary absorption are reduced.

Overall, these results are consistent with previous studies [13,35,51] and reinforce that, due to this effect, TiO_2 mortars showed less initial porosity. This decrease in the capillary absorp-

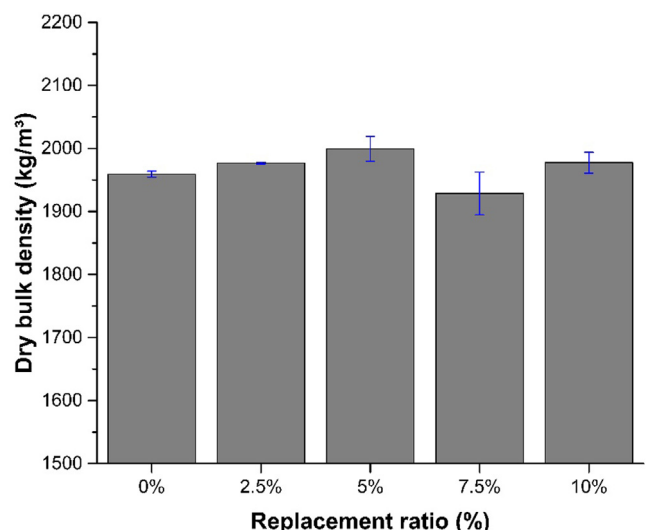


Fig. 4. Dry bulk density of hardened mortar.

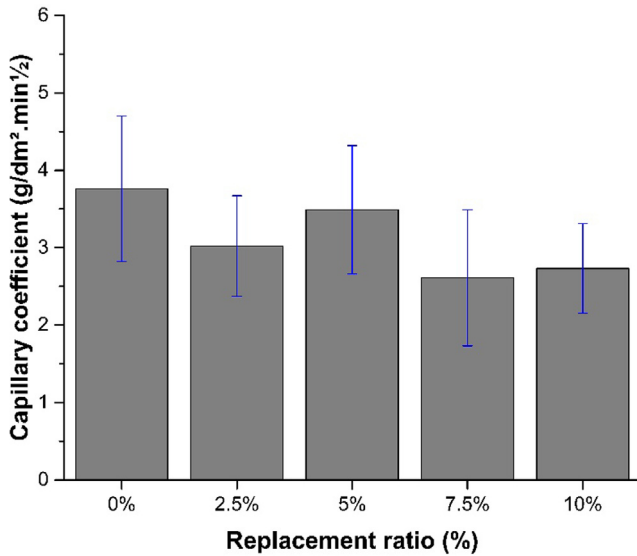


Fig. 5. Capillary coefficient of hardened mortar.

tion of mortars can indicate a significant improvement in the durability of cement mortars.

3.2.3. Open porosity

The volume of interconnected pores was estimated by the open porosity test and the results obtained are shown in Fig. 6. Based on the results, we observed that the extent to which TiO₂ was incorporated into open porosity also increased. This increase was not significant because the mortar with 10% TiO₂ (M4) showed an increase of only about 13% compared to the reference mortar (M0). The results are contrary to some previous studies [13,51] and indicate that the particle filling effect was not efficient for this property. This also shows that the effect of increasing the water/cement ratio affects the porosity of the matrix when the TiO₂ nanoparticles are incorporated, especially when their dosage is equivalent to 10%.

However, we observed that the water content increases when TiO₂ is incorporated (Table 1). Due to their larger specific surface, TiO₂ nanoparticles tend to agglomerate, leading to the formation of undisrupted pockets within the cementitious matrix [35]. As a result, mortars have a higher pore volume when hardened. These

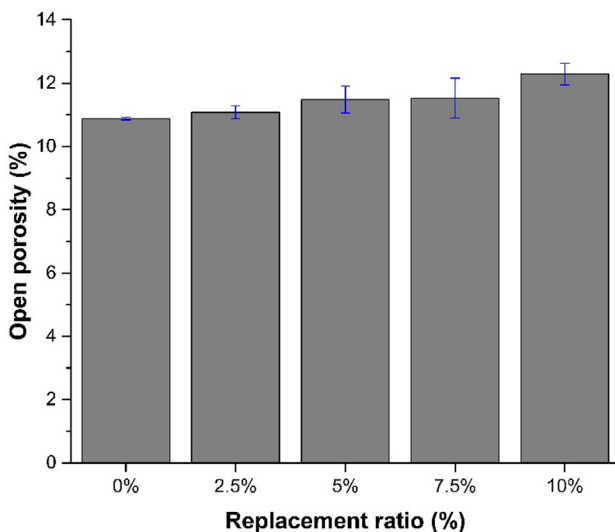


Fig. 6. Open porosity of hardened mortar.

results corroborate those obtained in previous studies [12,35] and, therefore, confirm that there may be a joint effect of pore size reduction and porosity increase for mortars that incorporate a higher amount of TiO₂ [12]. In the mortar study carried out by Atta-ur-Rehman et al. [30] it is observed that that water absorption is reduced when nano-TiO₂ is added. This was because the TiO₂ particles were first deagglomerated and dispersed in water through ultrasonication using a sonic probe for at least 45 min. Thus, dispersants or ultra-sound would be required for agitation in future studies to prevent the particle agglomeration phenomena.

Davood et al. [35] showed that when TiO₂ content is greater than 3.5% by weight, the total pore volume and the number of pores in mortars tend to increase. However, the high open porosity of mortars produced with TiO₂ may contribute to the better diffusion of CO₂ in the atmosphere, which is beneficial for the environment over time [52].

3.2.4. Flexural and compressive strength

The results obtained in the flexural and compressive strength tests at 7 and 28 days of moist curing can be seen in Fig. 7. It is observed that mortars have values of flexural strength greater than 3.5 MPa and compressive strength greater than 8 MPa. Comparing the results obtained with the compressive strength classes proposed in NP EN 998-1: 2013, it should be noted that all mortars studied belong to the CS III and CS IV classes, making them suitable for most applications. Regarding the Brazilian standardization (NBR 1281: 2005), mortars may be suitable to be used as monolayer decorative coating mortars.

In general, it can be observed that the replacement of PC by TiO₂ caused increased compressive and flexural strength of mortars. The filling effect of TiO₂ nanoparticles made mortars more compact and denser, which resulted in improved compressive strength. These results corroborate those obtained in other studies [13,31,35,51,53]. Notwithstanding, other factors may have contributed to this performance, such as the nucleation effect in the cement paste [13,35,51,53]. As a result, hydration products defuse and envelop nano-particles acting as a kernel, which leads to a better distribution of hydration products and stronger clusters of C-S-H [30]. These observations corroborate the results obtained in the analysis of the open porosity of mortars (Section 3.2.3).

3.3. Photocatalytic analysis

A great similarity between the FTIR spectra of the cement after incorporating sulfur dioxide (SO₂) was observed, as well as after

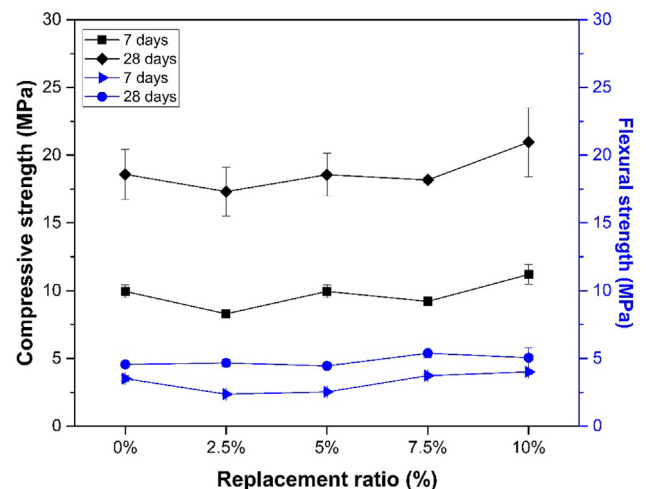


Fig. 7. Compressive and flexural strength of hardened mortars.

they were exposed to UV radiation (Figs. 8 and 9). The figures show the unpolluted mortar tablets (np), polluted with SO₂ (p) and after exposure to radiation (r). The presence of SO₂ in the cement can be confirmed by the appearance of absorption bands related to the S-O stretching, which are absent in the reference cement (M0). The main absorption bands and their assignments are summarized in Table 5.

The presence of SO₂ in the cement can be observed by the absorption band at 1140 cm⁻¹, which corresponds to the stretching of the S-O bond. According to the literature, when SO₂ is poorly adsorbed on a surface, bands appear between 1330 and

Table 5

Main absorption bands present in the FTIR spectra of cement mortars and their assignments.

Absorption band (cm ⁻¹)	Assignment	Reference
3400	ν (O - H)	[19,39,43]
1800	ν (Ti - O - Ti)	[40-42]
1640	δ (O - H)	[37,44]
1140	ν (S - O)	[36,38]
1090	ν_a (Si - O - Si)	[37,44,45]
870	ν_s (Si - O - Si)	[37,44,45]
470	δ (R ₃ Si - O - SiR ₃)	[37,44]
460	ν (Ti - O - Ti)	[40-42]

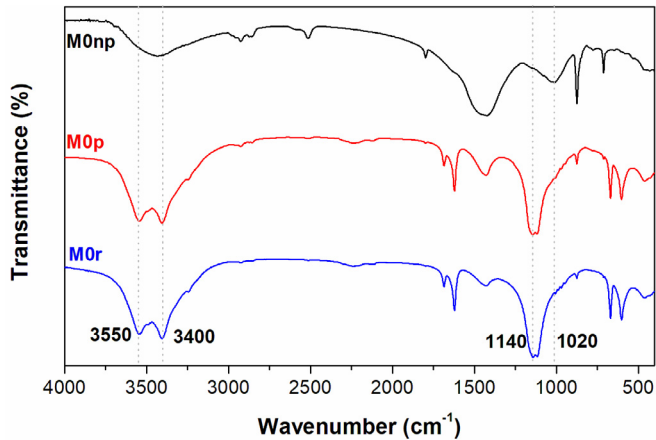
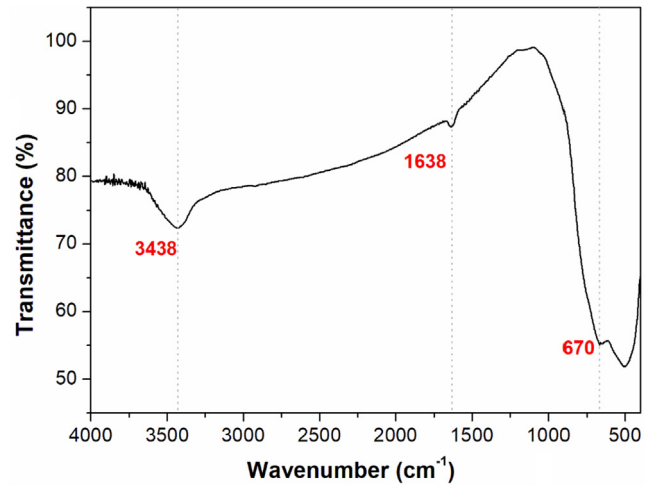
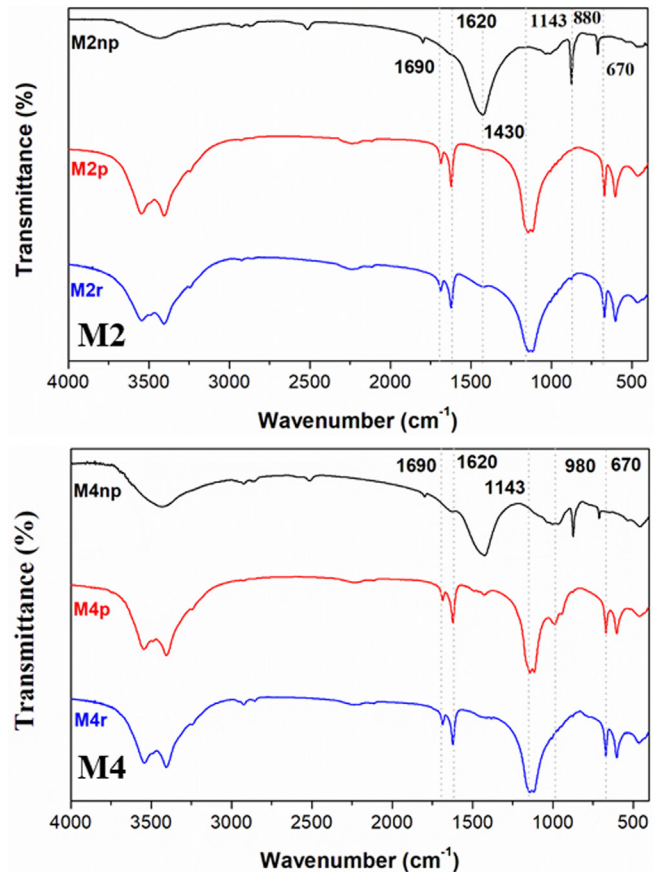
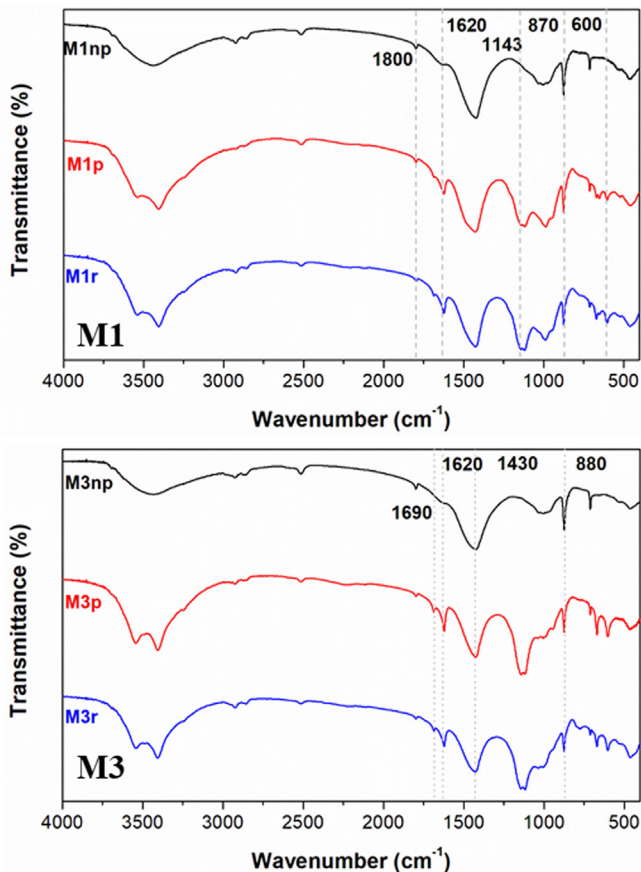


Fig. 8. FTIR spectrum of the reference cement.

Fig. 10. FTIR spectrum of TiO₂ (anatase phase).Fig. 9. FTIR spectrum of the cement incorporated with TiO₂.

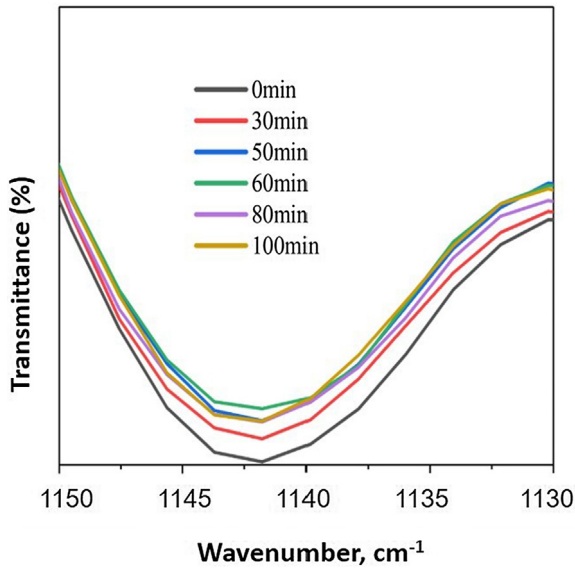


Fig. 11. FTIR spectra of reference cement (M0) for SO_2 release.

1140 cm^{-1} [36,38], which is consistent with the obtained spectra shown in Fig. 8.

The band at 3400 cm^{-1} can be attributed to symmetric stretching of hydroxyl groups, which can be present in the silanol groups

or those present in the adsorbed water molecules in the surface of the cement or by the reaction between the electron pairs, which in the photocatalysis reaction migrate to the catalyst surface and react separately with other species adsorbed to this surface, such as water [19,39,43]. The adsorption of water molecules on the surface of the catalyst acts by preventing polluting molecules from being adsorbed on the surface, which makes additional reactions with TiO_2 difficult or do not occur [28].

The bands at 1090 and 870 cm^{-1} are related to the asymmetric and symmetric stretching of Si-O-Si groups, respectively [37,44,45]. Furthermore, the bands at 470 cm^{-1} can be attributed to the angular deformation of siloxane groups, while the band at 1640 cm^{-1} can be attributed to the angular vibration of the adsorbed water molecules [37,44].

In addition, the incorporation of TiO_2 to the cement was successfully proved by the appearance of bands at 460 and 1800 cm^{-1} , which are related to the Ti-O and Ti-O-Ti stretching, respectively. The presence of a band at 480 cm^{-1} in the neat cement (M0) can also be observed, as well as in the cements with TiO_2 . This behavior can be explained by the fact that the SiO_2 groups also absorb the radiation in this region. Moreover, when TiO_2 (anatase) is strongly adsorbed, it will produce an absorption band at 480 cm^{-1} which is related to the stretching of the O-Ti-O bond [40-42], as shown in Fig. 10.

Figs. 11 and 12 show the FTIR spectra of the neat cement (M0) and the cements with TiO_2 (M1, M2, M3 and M4), respectively, in which the release behavior of SO_2 was monitored. The figures showed that there was no tendency to release sulfur for all formu-

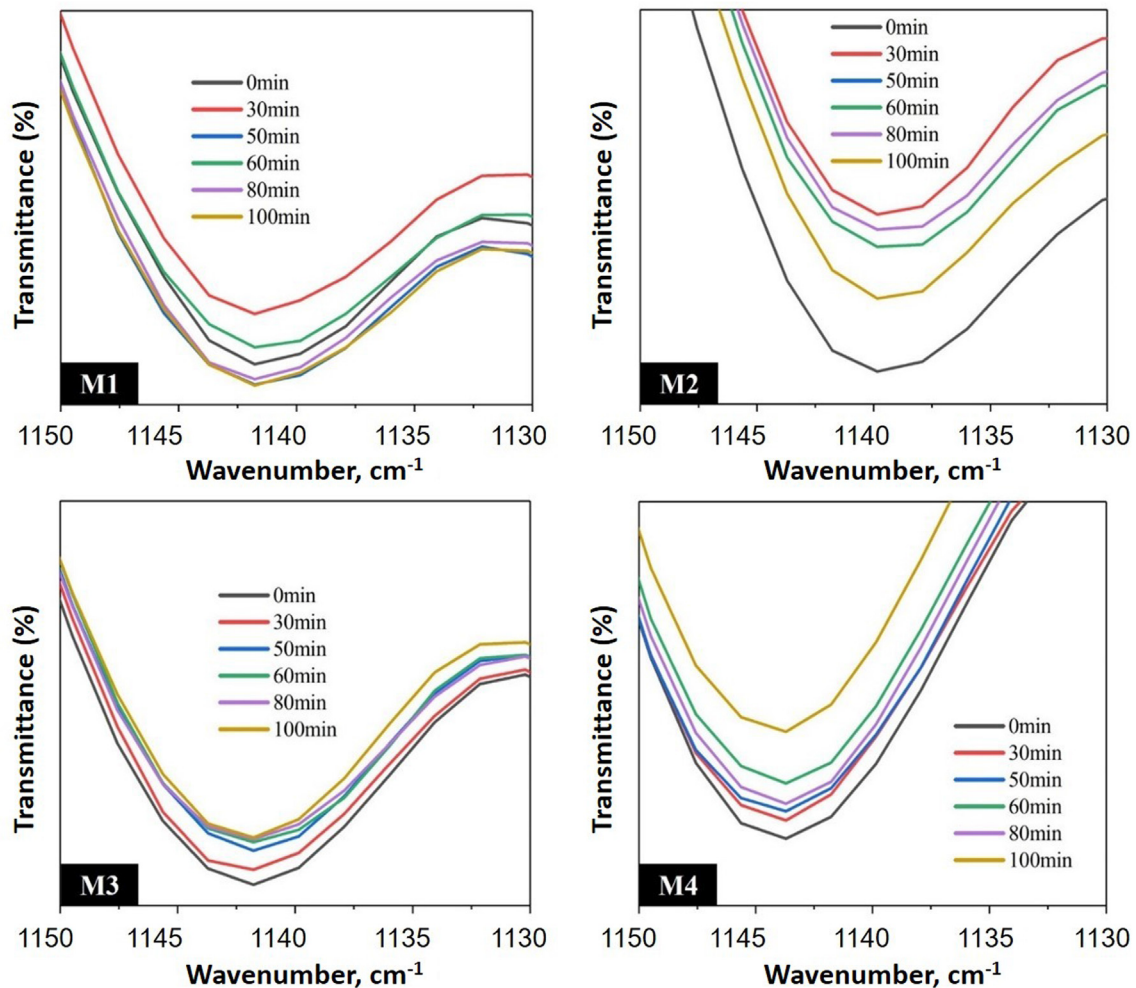
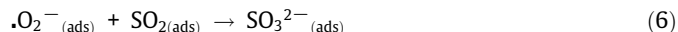
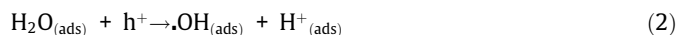


Fig. 12. FTIR spectra of cements with TiO_2 (M1, M2, M3 and M4) for SO_2 release.

lations/compositions. The degradation mechanism of SO₂ was proposed in the following Equations (1 to 6), based on a previous pathway proposed by Chen and Kou [54].



TiO₂ nanoparticles are activated by the incidence of UV light in cement mortars, creating a gap (h⁺) in the valence band (VB) and releasing an electron (e⁻) to the conduction band (CB). Water molecules present in the atmosphere can be adsorbed on the cement mortar' surface as previously shown by FTIR spectra (Eq. (1)) and can undergo an oxidation reaction in the VB producing hydroxyl radicals (·OH) (Eq. (2)), which are highly reactive. Oxygen molecules also present in the air can undergo a reduction reaction in the CB producing superoxide species (·O₂⁻) (Eq. (3)), which are also highly reactive. Then, SO₂ molecules in the air can be adsorbed on the cement mortar' surface (Eq. (4)), reacting with the reactive oxygen species, such as ·OH and ·O₂⁻, producing sulfite (SO₃²⁻) and sulfate (SO₄²⁻) ions (Eqs. (5) and (6)), respectively, which are less polluting and aggressive species than SO₂.

When the behavior of M0 is observed, we notice that there is no tendency to release sulfur. It can be concluded that this is due to the fact that there is practically no distance from the curves over time. When we analyze mortars with TiO₂ nanoparticles, we see another configuration (there is a reduction trend, mainly of M2).

Fig. 12 clearly shows that the transmittance of the bands related to the S-O bond decreased faster in the cements with TiO₂ (M1 to M4) than those of the neat cement (M0). This can be related to the kinetics involved in the SO₂ release, indicating that the incorporation of TiO₂ particles to the cement combined to the exposure to the radiation catalyzed the release process, in which the M2 and M4 samples had the highest weight loss, specifically 1.5% wt. only during 100 min of exposure. Therefore, these results show the potential of using low contents of TiO₂ for obtaining fast and efficient responses in relation to SO₂ release, minimizing several environmental problems, as well as the deterioration of the cement.

4. Conclusion

It can be concluded from this study that the introduction of nano TiO₂ helped to improve the photocatalytic properties of the mortars. As the radiation exhibition time increases, the intensity of the adsorption band in the SO₂ region is reduced. Thus, the reduced SO₂ content in the mortars was observed, demonstrating that there was sulfur release from the made samples. Reduction is a positive factor for achieving sustainability in construction, through non-polluting materials that still act to provide greater durability to buildings. The results obtained from the physical properties show that it is feasible to use mortars with TiO₂ incorporation in decorative monolayer coating on facades. The reduction in SO₂ of the samples is due to the increase in its porosity. Notwithstanding, it is interesting to note that better results of physical properties probably could have been obtained when using ultrasonication using a sonic probe to de-agglomerate and disperse nano-TiO₂ particles in water instead of incorporating the fines (nanoparticles and cement) together.

CRediT authorship contribution statement

C. N. Fernandes: Conceptualization, Data curation, Formal analysis, Investigation, Methodology, Writing - original draft, Writing - review & editing. **R. L. S. Ferreira:** Formal analysis, Software, Validation, Writing - original draft, Writing - review & editing. **R. D. S. Bernardo:** Conceptualization, Data curation, Formal analysis, Investigation, Methodology, Validation, Writing - review & editing. **F. Avelino:** Formal analysis, Software, Validation, Writing - review & editing. **A. A. Bertini:** Conceptualization, Funding acquisition, Project administration, Resources, Supervision, Visualization.

Declaration of Competing Interest

The authors declare that they have no known competing financial interests or personal relationships that could have appeared to influence the work reported in this paper.

Acknowledgements

We would like to thank the Building Materials Laboratory from the Federal Institute of Education, Science and Technology of Rio Grande do Norte and the Bioinorganic Laboratory from the Federal University of Ceará, for the support during the development of this study and CAPES for granting the scholarship.

References

- [1] S. Armenta M. de la Guardia Pollutants and Air Pollution, in 2016 10.1016/bs.coac.2016.03.002 27 44
- [2] J. Fenger, Air pollution in the last 50 years - From local to global, Atmos. Environ. 43 (2009) 13-22, <https://doi.org/10.1016/j.atmosenv.2008.09.061>.
- [3] J. Fenger, Urban air quality, in: J. Austin, P. Brimblecombe, W. Struges (Eds.), Air Pollut. Sci. 21st Century, Elsevier S, 2002: pp. 1-52. [https://doi.org/10.1016/S1474-8177\(02\)80004-3](https://doi.org/10.1016/S1474-8177(02)80004-3).
- [4] World Health Organization Regional Office for Europe, Health aspects of air pollution with particulate matter, ozone and nitrogen dioxide 2003 Germany
- [5] S.P. Santos, A.P. Duarte, J.C. Bordado, J.F. Gomes, New process for simultaneous removal of CO₂, SO_x and NO_x, Ciênc. Tecnol. Dos Mater. 28 (2016) 106-111, <https://doi.org/10.1016/j.ctmat.2016.12.002>.
- [6] A. Zeng, X. Mao, T. Hu, Y. Xing, Y. Gao, J. Zhou, Y. Qian, Regional co-control plan for local air pollutants and CO₂ reduction: Method and practice, J. Clean. Prod. 140 (2017) 1226-1235, <https://doi.org/10.1016/j.jclepro.2016.10.037>.
- [7] X. Chen, S. Shao, Z. Tian, Z. Xie, P. Yin, Impacts of air pollution and its spatial spillover effect on public health based on China's big data sample, J. Clean. Prod. 142 (2017) 915-925, <https://doi.org/10.1016/j.jclepro.2016.02.119>.
- [8] A.J. Haider, Z.N. Jameel, I.H.M. Al-Hussaini, Review on: Titanium Dioxide Applications, Energy Procedia. 157 (2019) 17-29, <https://doi.org/10.1016/j.egypro.2018.11.159>.
- [9] X. Tang L. Ughetta S.K. Shannon S. Houzé de l'Aulnoit, S. Chen, R.A.T. Gould, M. L. Russell, J. Zhang, G. Ban-Weiss, R.L.A. Everman, F.W. Klink, R. Levinson, H. Destailats, De-pollution efficacy of photocatalytic roofing granules Build. Environ. 160 2019 106058 10.1016/j.buildenv.2019.03.056
- [10] M.-Z. Guo, T.-C. Ling, C.S. Poon, Photocatalytic NO_x degradation of concrete surface layers intermixed and spray-coated with nano-TiO₂: Influence of experimental factors, Cem. Concr. Compos. 83 (2017) 279-289, <https://doi.org/10.1016/j.cemconcomp.2017.07.022>.
- [11] D.F. Ollis, E. Pelizzetti, N. Serpone, Photocatalyzed destruction of water contaminants, Environ. Sci. Technol. 25 (1991) 1522-1529, <https://doi.org/10.1021/es00021a001>.
- [12] S.S. Lucas, V.M. Ferreira, J.L.B. de Aguiar, Incorporation of titanium dioxide nanoparticles in mortars - Influence of microstructure in the hardened state properties and photocatalytic activity, Cem. Concr. Res. 43 (2013) 112-120, <https://doi.org/10.1016/j.cemconres.2012.09.007>.
- [13] J.H. Atta-ur-Rehman, H.G. Kim, A. Kim, J.-S. Qudoos, Ryou, Effect of leaching on the hardened, microstructural and self-cleaning characteristics of titanium dioxide containing cement mortars, Constr. Build. Mater. 207 (2019) 640-650, <https://doi.org/10.1016/j.conbuildmat.2019.02.170>.
- [14] A. Fujishima, T.N. Rao, D.A. Tryk, Titanium dioxide photocatalysis, J. Photochem. Photobiol. C Photochem. Rev. 1 (2000) 1-21, [https://doi.org/10.1016/S1389-5567\(00\)00002-2](https://doi.org/10.1016/S1389-5567(00)00002-2).
- [15] M.A. Henderson, A surface science perspective on TiO₂ photocatalysis, Surf. Sci. Rep. 66 (2011) 185-297, <https://doi.org/10.1016/j.surfrep.2011.01.001>.
- [16] M. Bellardita, A. Di Paola, B. Megna, L. Palmisano, Determination of the crystallinity of TiO₂ photocatalysts, J. Photochem. Photobiol. A Chem. 367 (2018) 312-320, <https://doi.org/10.1016/j.jphotochem.2018.08.042>.

- [17] L. Liu, H. Zhao, J.M. Andino, Y. Li, Photocatalytic CO₂ Reduction with H₂O on TiO₂ Nanocrystals: Comparison of Anatase, Rutile, and Brookite Polymorphs and Exploration of Surface Chemistry, *ACS Catal.* 2 (2012) 1817–1828, <https://doi.org/10.1021/cs300273q>.
- [18] R.C. Bhave, B.I. Lee, Experimental variables in the synthesis of brookite phase TiO₂ nanoparticles, *Mater. Sci. Eng. A.* 467 (2007) 146–149, <https://doi.org/10.1016/j.msea.2007.02.092>.
- [19] V. Etacheri, C. Di Valentin, J. Schneider, D. Bahnemann, S.C. Pillai, Visible-light activation of TiO₂ photocatalysts: Advances in theory and experiments, *J. Photochem. Photobiol. C Photochem. Rev.* 25 (2015) 1–29, <https://doi.org/10.1016/j.jphotochemrev.2015.08.003>.
- [20] A.L. Linsebigler, G. Lu, J.T. Yates, Photocatalysis on TiO₂ Surfaces: Principles, Mechanisms, and Selected Results, *Chem. Rev.* 95 (1995) 735–758, <https://doi.org/10.1021/cr00035a013>.
- [21] M. Stamate, G. Lazar, Application of titanium dioxide photocatalysis to create selfcleaning materials, *Rom. Tech. Sci. Acad.* 3 (2007) 280–285.
- [22] G. Qian, H. Yu, X. Gong, L. Zhao, Impact of Nano-TiO₂ on the NO₂ degradation and rheological performance of asphalt pavement, *Constr. Build. Mater.* 218 (2019) 53–63, <https://doi.org/10.1016/j.conbuildmat.2019.05.075>.
- [23] X. Zhu, W. Yuan, M. Lang, G. Zhen, X. Zhang, X. Lu, Novel methods of sewage sludge utilization for photocatalytic degradation of tetracycline-containing wastewater, *Fuel.* 252 (2019) 148–156, <https://doi.org/10.1016/j.fuel.2019.04.093>.
- [24] B. Forsthuber, U. Müller, A. Teischinger, G. Grüll, Chemical and mechanical changes during photooxidation of an acrylic clear wood coat and its prevention using UV absorber and micronized TiO₂, *Polym. Degrad. Stab.* 98 (2013) 1329–1338, <https://doi.org/10.1016/j.polymdegradstab.2013.03.029>.
- [25] A. Fujishima, X. Zhang, Titanium dioxide photocatalysis: present situation and future approaches, *Comptes Rendus Chim.* 9 (2006) 750–760, <https://doi.org/10.1016/j.crci.2005.02.055>.
- [26] M.V. Diamanti, R. Paolini, M. Rossini, A.B. Aslan, M. Zinzi, T. Poli, M.P. Pedferri, Long term self-cleaning and photocatalytic performance of anatase added mortars exposed to the urban environment, *Constr. Build. Mater.* 96 (2015) 270–278, <https://doi.org/10.1016/j.conbuildmat.2015.08.028>.
- [27] G.G. Guillén, S. Shaji, M.I.M. Palma, D. Avellaneda, G.A. Castillo, T.K. Das Roy, D. I.G. Gutiérrez, B. Krishnan, Effects of ablation energy and post-irradiation on the structure and properties of titanium dioxide nanomaterials, *Appl. Surf. Sci.* 405 (2017) 183–194, <https://doi.org/10.1016/j.apsusc.2017.01.282>.
- [28] G. Hüskén, M. Hunger, H.J.H. Brouwers, Experimental study of photocatalytic concrete products for air purification, *Build. Environ.* 44 (2009) 2463–2474, <https://doi.org/10.1016/j.buildenv.2009.04.010>.
- [29] A. Jerónimo, A. Camões, B. Aguiar, N. Lima, Hydraulic lime mortars with antifungal properties, *Appl. Surf. Sci.* 483 (2019) 1192–1198, <https://doi.org/10.1016/j.apsusc.2019.03.156>.
- [30] A. Atta-ur-Rehman, H.G. Qudoos, J.-S. Kim, Ryou, Influence of Titanium Dioxide Nanoparticles on the Sulfate Attack upon Ordinary Portland Cement and Slag-Blended Mortars, *Materials (Basel)*. 11 (2018) 356, <https://doi.org/10.3390/ma11030356>.
- [31] A. Nazari, S. Riahi, The effect of TiO₂ nanoparticles on water permeability and thermal and mechanical properties of high strength self-compacting concrete, *Mater. Sci. Eng. A.* 528 (2010) 756–763, <https://doi.org/10.1016/j.msea.2010.09.074>.
- [32] A. Atta-ur-Rehman, S.H. Qudoos, H.G. Jakhriani, J.-S. Kim, Ryou, Influence of Nano-silica on the Leaching Attack upon Photocatalytic Cement Mortars, *Int. J. Concr. Struct. Mater.* 13 (2019) 35, <https://doi.org/10.1186/s40069-019-0348-x>.
- [33] Atta-ur-Rehmana, Jae-Suk Ryou, Sadam Hussain Jakhriani, Hong-Gi Kim, Jeong Bae Lee, Abdul Qudoos, Influence of nano silica on the fresh, hardened and durability properties of self-cleaning white Portland cement mortars, *J. Ceram. Process. Res.* 20 (2019) 270–275, <https://doi.org/10.36410/jcpr.2019.20.3.270>.
- [34] D. Feng, N. Xie, C. Gong, Z. Leng, H. Xiao, H. Li, X. Shi, Portland Cement Paste Modified by TiO₂ Nanoparticles: A Microstructure Perspective, *Ind. Eng. Chem. Res.* 52 (2013) 11575–11582, <https://doi.org/10.1021/ie4011595>.
- [35] D. Shafaei, S. Yang, L. Berliouis, J. Minto, Multiscale pore structure analysis of nano titanium dioxide cement mortar composite, *Mater. Today Commun.* 22 (2020), <https://doi.org/10.1016/j.mtcomm.2019.100779>.
- [36] J. Zawadzki, Infrared studies of SO₂ on carbons—I. Interaction of SO₂ with carbon films, *Carbon N. Y.* 25 (1987) 431–436, [https://doi.org/10.1016/0008-6223\(87\)90015-7](https://doi.org/10.1016/0008-6223(87)90015-7).
- [37] J.A.A. Sales, F.P. Faria, A.G.S. Prado, C. Airoidi, Attachment of 2-aminomethylpyridine molecule onto grafted silica gel surface and its ability in chelating cations, *Polyhedron.* 23 (2004) 719–725, <https://doi.org/10.1016/j.poly.2003.11.051>.
- [38] G. Ramakrishnan, Q. Wu, J. Moon, A. Orlov, Reactions of SO₂ on hydrated cement particle system for atmospheric pollution reduction: A DRIFTS and XANES study, *Chem. Eng. J.* 319 (2017) 57–64, <https://doi.org/10.1016/j.cej.2017.02.135>.
- [39] X. Chen, D.-H. Kuo, D. Lu, N-doped mesoporous TiO₂ nanoparticles synthesized by using biological renewable nanocrystalline cellulose as template for the degradation of pollutants under visible and sun light, *Chem. Eng. J.* 295 (2016) 192–200, <https://doi.org/10.1016/j.cej.2016.03.047>.
- [40] S. Liu, W. Wang, J. Chen, J.-G. Li, X. Li, X. Sun, Y. Dong, Foamed single-crystalline anatase nanocrystals exhibiting enhanced photocatalytic activity, *J. Mater. Chem. A.* 3 (2015) 17837–17848, <https://doi.org/10.1039/C5TA04682C>.
- [41] S. Deivanayaki, V. Ponnuswamy, S. Ashokan, P. Jayamurugan, R. Mariappan, Synthesis and characterization of TiO₂-doped Polyaniline nanocomposites by chemical oxidation method, *Mater. Sci. Semicond. Process.* 16 (2013) 554–559, <https://doi.org/10.1016/j.mssp.2012.07.004>.
- [42] L. Gu, J. Wang, R. Qi, X. Wang, P. Xu, X. Han, A novel incorporating style of polyaniline/TiO₂ composites as effective visible photocatalysts, *J. Mol. Catal. A Chem.* 357 (2012) 19–25, <https://doi.org/10.1016/j.molcata.2012.01.012>.
- [43] I. Daou, O. Zegaoui, A. Elghazouani, Physicochemical and photocatalytic properties of the ZnO particles synthesized by two different methods using three different precursors, *Comptes Rendus Chim.* 20 (2017) 47–54, <https://doi.org/10.1016/j.crci.2016.04.003>.
- [44] F.G. Doro, U.P. Rodrigues-Filho, E. Tfouni, A regenerable ruthenium tetraammine nitrosyl complex immobilized on a modified silica gel surface: Preparation and studies of nitric oxide release and nitrite-to-NO conversion, *J. Colloid Interface Sci.* 307 (2007) 405–417, <https://doi.org/10.1016/j.jcis.2006.11.013>.
- [45] R. Fateh, R. Dillert, D. Bahnemann, Preparation and Characterization of Transparent Hydrophilic Photocatalytic TiO₂/SiO₂ Thin Films on Polycarbonate, *Langmuir.* 29 (2013) 3730–3739, <https://doi.org/10.1021/la400191x>.
- [46] P. Sikora, K. Cendrowski, A. Markowska-Szczupak, E. Horszczaruk, E. Mijowska, The effects of silica/titania nanocomposite on the mechanical and bactericidal properties of cement mortars, *Constr. Build. Mater.* 150 (2017) 738–746, <https://doi.org/10.1016/j.conbuildmat.2017.06.054>.
- [47] J. Chen, S. Kou, C. Poon, Photocatalytic cement-based materials: Comparison of nitrogen oxides and toluene removal potentials and evaluation of self-cleaning performance, *Build. Environ.* 46 (2011) 1827–1833, <https://doi.org/10.1016/j.buildenv.2011.03.004>.
- [48] E. Franzoni, A. Fregni, R. Gabrielli, G. Graziani, E. Sassoni, Compatibility of photocatalytic TiO₂-based finishing for renders in architectural restoration: A preliminary study, *Build. Environ.* 80 (2014) 125–135, <https://doi.org/10.1016/j.buildenv.2014.05.027>.
- [49] R.H. Keates, D.E. Genstler, UV radiation, United States Environ. Prot. Agency. (2010). https://doi.org/10.1007/978-3-662-46875-3_6139.
- [50] J.M. da Silveira Carvalho, A.H. de Morais Batista, N.A.P. Nogueira, A.K.M. Holanda, J.R. de Sousa, D. Zampieri, M.J.B. Bezerra, F. Stefânio Barreto, M.O. de Moraes, A.A. Batista, A.C.S. Gondim, T.F. dePaulo, L.G. de França Lopes, E.H.S. Sousa, A bisphosphinic ruthenium complex with potent anti-bacterial and anti-cancer activity, *New J. Chem.* 41 (2017) 13085–13095, <https://doi.org/10.1039/C7NJ02943H>.
- [51] H. Noorvand, A.A. Abang Ali, R. Demirboga, N. Farzadnia, H. Noorvand, Incorporation of nano TiO₂ in black rice husk ash mortars, *Constr. Build. Mater.* 47 (2013) 1350–1361, <https://doi.org/10.1016/j.conbuildmat.2013.06.066>.
- [52] R.L.S. Ferreira, M.A.S. Anjos, A.K.C. Nóbrega, J.E.S. Pereira, E.F. Ledesma, The role of powder content of the recycled aggregates of CDW in the behaviour of rendering mortars, *Constr. Build. Mater.* 208 (2019), <https://doi.org/10.1016/j.conbuildmat.2019.03.058>.
- [53] L.Y. Yang, Z.J. Jia, Y.M. Zhang, J.G. Dai, Effects of nano-TiO₂ on strength, shrinkage and microstructure of alkali activated slag pastes, *Cem. Concr. Compos.* 57 (2015) 1–7, <https://doi.org/10.1016/j.cemconcomp.2014.11.009>.
- [54] X.-F. Chen, S.-C. Kou, Sulfur Dioxide Degradation by Composite Photocatalysts Prepared by Recycled Fine Aggregates and Nanoscale Titanium Dioxide, *Nanomaterials.* 9 (2019) 1533, <https://doi.org/10.3390/nano9111533>.



SERVIÇO PÚBLICO FEDERAL
MINISTÉRIO DA EDUCAÇÃO
SECRETARIA DE EDUCAÇÃO PROFISSIONAL E TECNOLÓGICA
INSTITUTO FEDERAL DE EDUCAÇÃO, CIÊNCIA E TECNOLOGIA DE PERNAMBUCO
CAMPUS PESQUEIRA

COORDENAÇÃO DA ÁREA DE CONSTRUÇÃO CIVIL - CACC

DECLARAÇÃO

Declaro para comprovação junto ao IFPE que os professores citados na tabela abaixo, foram designados na continuidade emergencial da Portaria Nº 057/2014 – DGCP, visto uma demanda de caráter da PRODEN.

Docentes	Siape
ELÂNIA DE SOUZA MELO	1650623
ISNARD FERREIRA DA SILVA	1204757
JAQUELINE MATIAS DA SILVA	1397823
JOSE DENIS GOMES LIMA DA SILVA	1971579
MANUELA QUEIROZ OLIVEIRA	2891298
MARIO JOSE RIBEIRO DA SILVA	1216014
RAFAEL RONEY CAMARA DE MELO	1959798
RICARDO GOMES FREIRE DUARTE	3131891
RONALDO ALVES DE OLIVEIRA FILHO	2961669
RUAN LANDOLFO FERREIRA DA SILVA	3087909

Pesqueira, 13 de novembro de 2020.



Documento assinado digitalmente
Jose Denis Gomes Lima da Silva
Data: 13/11/2020 11:09:56-0300
CPF: 048.249.324-08

José Denis Gomes Lima da Silva / Siape 1971579
Coordenador da Área de Construção Civil
IFPE Campus Pesqueira



INSTITUTO FEDERAL DE EDUCAÇÃO CIÊNCIA E TECNOLOGIA DE PERNAMBUCO

CNPJ 02.816.789/0001-89 – Decreto S/N de 18/01/1999

Autorizado a funcionar de acordo com a portaria do MEC nº 1.533 de 19/10/1992

Rodovia BR 232 Km 214 – Prado – Pesqueira – PE – Telefax: 87 3835-1796

DEX – DEPARTAMENTO DE EXTENSÃO

CEEG – COORDENAÇÃO DE ESTÁGIOS E EGRESSOS

DECLARAÇÃO

Declaramos para fins de direito que o professor **Ruan Landoufo da Silva Ferreira, Siape 3087909**, exerceu a função de orientador de estágio no curso Técnico em Edificações desta Instituição de Ensino no semestre de 2020.1 nos seguintes termos:

<i>Aluno</i>	<i>Matrícula</i>
Ana Beatriz Nunes Leal	20182A2-PS0170
Marcos Antônio Tenório de Almeida Filho	20151A12-PS0026

Pesqueira, 16 de Novembro de 2020.

Rafael Roney Camara de Melo

Siape 1959798

Coordenação de Estágios e Egressos – IFPE Campus Pesqueira

Portaria D.O.U. nº55 de 11/01/2018



Documento assinado digitalmente

Rafael Roney Camara de Melo
Data: 16/11/2020 08:34:20-0300
CPF: 072.863.264-06



INSTITUTO FEDERAL DE EDUCAÇÃO CIÊNCIA E TECNOLOGIA DE PERNAMBUCO

CNPJ 02.816.789/0001-89 – Decreto S/N de 18/01/1999

Autorizado a funcionar de acordo com a portaria do MEC nº 1.533 de 19/10/1992

Rodovia BR 232 Km 214 – Prado – Pesqueira – PE – Telefax: 87 3835-1796

DEPARTAMENTO DE EXTENSÃO - DEX

DECLARAÇÃO

Declaro para fins de direito e comprovação que o servidor **RUAM LANDOLFO DA SILVA FERREIRA**, matrícula SIAPE: 3087909, é colaborador interno no projeto de extensão aprovado no Edital Nº 01/2019 – PIBEX/PROEXT/IFPE, com o título “**DESENVOLVIMENTO SUSTENTÁVEL NAS CONSTRUÇÕES DO POVO INDÍGENA XUKURU DO ORORUBÁ: ENSINO E APRENDIZAGEM POR MEIO DE REGISTROS E INFORMAÇÕES DO POVO XUKURU - VISITAS TÉCNICAS E CARACTERIZAÇÃO DOS MATERIAIS DA CONSTRUÇÃO CIVIL**”, cadastrado neste Departamento de Extensão e que vem sendo executado de fevereiro de 2020 até a presente data, exercendo uma carga horária semanal de 02h.

Pesqueira-PE, 16 de novembro de 2020.

Documento assinado digitalmente

gov.br

Otávio Washington Lima Silva
Data: 16/11/2020 09:11:54-0300
CPF: 095.354.834-12

Otávio Washington Lima Silva
Departamento de Extensão/IFPE – Campus Pesqueira
Portaria DOU Nº 726/2019
Mat. SIAPE 2279405